Proceedings of the DIS'2004, Štrbské Pleso, Slovakia

SCALING VIOLATIONS OF QUARK AND GLUON JET FRAGMENTATION FUNCTIONS IN E^+E^- ANNIHILATIONS

MAREK TAŠEVSKÝ
Physics Department of the Antwerp University
Universiteitsplein 1, B-2610 Antwerp, Belgium

Flavour inclusive, udsc and b fragmentation functions in biased and unbiased jets and gluon fragmentation functions in biased jets are measured in e^+e^- annihilations using OPAL data collected at energies $\sqrt{s} = 91.2$ and 183–209 GeV.

1 Introduction

Hadron production in high energy collisions can be described by parton showers, followed by the formation of hadrons which cannot be described perturbatively. Gluon emission, the dominant process in parton showers, is proportional to the colour factor associated with the coupling of the emitted gluon to the emitter. These colour factors are $C_A = 3$ when the emitter is a gluon and $C_F = 4/3$ when it is a quark. Consequently, the multiplicity of soft gluons from a gluon source is (asymptotically) 9/4 times higher than from a quark source [1]. The inequality between C_A and C_F plays a key role in the explanation of the observed differences between quark and gluon jets: compared to quark jets, gluon jets are observed to have larger widths [2], higher multiplicities [2,3], softer fragmentation functions [2,4,5], and stronger scaling violations of the fragmentation functions [5].

The fragmentation function, $D_a^h(x, Q^2)$, is defined as the probability that parton a, which is produced at short distance, of order $1/Q$, fragments into hadron, h, carrying the fraction x of the momentum of a. In this study, the momentum fraction is defined as $x_{\mathrm{E}} = E_h/E_{\mathrm{j}et}$, where E_h is the energy of the hadron h and $E_{\mathrm{j}et}$ is the energy of the jet to which it is assigned.

Three-jet $\mathrm{q}\bar{q}\mathrm{g}$ events are selected by applying a jet finder. Different jet finders result in different assignments of particles to jets: thus jets defined using a jet finding algorithm are called *biased*. In contrast, quark and gluon jets used in theoretical calculations are usually defined as inclusive hemispheres of back-to-back $\mathrm{q}\bar{q}$ and gg final states, respectively. The hemisphere definition yields a so-called *unbiased* jet because the jet properties do not depend on the choice of a jet finder. Measurements of unbiased quark jets have been performed at many scales [6,7,8]. Direct measurements of unbiased gluon jets are so far available only from the CLEO [9] and OPAL [4,10] experiments, however. Recently, the OPAL experiment has measured properties of unbiased gluon jets indirectly [11,12].

In our study, we present measurements of quark and gluon jet fragmentation functions at $\sqrt{s} = 91.2$ GeV and $\sqrt{s} = 183$–209 GeV. The data were collected with the OPAL detector at the LEP e^+e^- collider at CERN. We measured seven types of fragmentation functions: those from biased as well as unbiased flavour inclusive, udsc and b jets, and from biased gluon jets. While the two types of flavour inclusive jets have been measured many times, data on the other types of fragmentation functions are still rather scarce.

2 Analysis procedure

The selection of hadronic Z and Z^*/γ^* events and any other details of this analysis are described in [13]. In the inclusive hadronic event samples, we use the unbiased jet definition where the jets are defined by particles in hemispheres of the $q\bar{q}$ system. In the three-jet samples, we apply a jet algorithm and thus work with biased jets. Three jet algorithms are used: the Durham [14], Cambridge [15] and cone [16] algorithms. The jet algorithm is forced to resolve three jets per event. The jet energies and momenta are then recalculated by imposing overall energy-momentum conservation with planar massless kinematics, using the jet directions found by the jet algorithm.

The measured fragmentation function is defined here as the total number of charged particles, N_p, in bins of $x_{\rm E}$ and scale Q normalized to the number of jets, $N_{jet}(Q)$, in the bin of Q:

$$\frac{1}{N_{jet}(Q)}\frac{\mathrm{d}N_p(x_{\rm E},Q)}{\mathrm{d}x_{\rm E}} \tag{1}$$

To measure the scale dependence, it is necessary to specify a scale relevant to the process under study. For inclusive hadronic events, the scale is $\sqrt{s}$. For jets in three-jet events, neither $\sqrt{s}$ nor E_{jet} is considered to be an appropriate choice of the scale [17]. QCD coherence suggests [18] that the event topology should also be taken into account. Similarly to previous studies, the transverse momentum-like scale, $Q_{jet} = E_{jet}\sin(\vartheta/2)$, is used where ϑ is the angle between the jet with E_{jet} and the closest other jet.

In this analysis, three methods are used to identify quark and gluon jets: the b-tag and the energy-ordering methods in biased three-jet events, and the hemisphere method in unbiased inclusive hadronic events. In addition, b tagging is used to separate udsc and b quark jets from each other, both for the biased and unbiased jet samples. The energy-ordering method only allows flavour inclusive quark jets to be distinguished from gluon jets.

All three methods are in detail described in [13]. In three-jet events, any of the three jets is used to extract the fragmentation functions. The purity of the b-tag (gluon) jet sample in LEP1 data is estimated to be 90% (84%) and the efficiencies are 23% (40%). The corresponding purities in LEP2 data are 60% (80%) and efficiencies 27% (45%). The purity of the b-tag hemispheres in LEP1 data is estimated to be 99.7%, while in LEP2 data it is 75%.

After subtracting the remaining background from LEP2 data using MC estimates, the data and MC distributions at detector level are multiplied by corresponding inverse matrices to get the distributions at level of pure quarks and gluons. As a last step, the data are corrected for effects of limited detector acceptance and resolution using correction factors obtained from MC events.

3 Results

The measured fragmentation functions are presented with emphasis on the scale dependence (the x_{E} dependence and other comparisons are shown in [13]) and are compared with previous measurements as well as with theoretical NLO predictions. The term scale in the following figures stands for $Q_{\mathrm{j}et}$ in case of biased jets and $\sqrt{s}/2$ in case of unbiased jets. The published unbiased jet results and the NLO predictions are scaled by $\frac{1}{2}$ since they refer to the entire event, thus to two jets.

In Figs. 1a)–d) the results for the udsc, b, gluon and flavour inclusive jet fragmentation functions are presented. The LEP1 unbiased jet data correspond to $\sqrt{s} = 91.2$ GeV. The LEP2 unbiased b jets are measured in $\sqrt{s}$ range of 183–209 GeV, while the unbiased udsc and flavour inclusive jets are measured in three $\sqrt{s}$ intervals: 183–189, 192–202 and 204–209 GeV. The quark biased jet data from LEP1 cover the region $Q_{\mathrm{j}et} =$ 4–42 GeV, while those from LEP2 cover the region $Q_{\mathrm{j}et} =$ 30–105 GeV. The results from the region $0.01 < x_{\mathrm{E}} < 0.03$ are not shown but they are presented in [13]. As also discussed in [13], the results are found to be consistent with previous measurements. The udsc jet results above 45.6 GeV, the gluon jet results above 30 GeV (except for the g_{incl} jets, see [4]), and the b jet results at all scales except 45.6 GeV represent the first measurements.

The data are compared to three theoretical predictions: Kniehl, Kramer and Pötter (KKP) [19], Kretzer (Kr) [20] and Bourhis, Fontannaz, Guillet and Werlen (BFGW) [21]. For the udsc jet fragmentation function (Fig. 1a)), all three predictions give a good description in the entire measured phase space, except for the lowest x_{E} bin where the KKP calculations overestimate the data, and the highest x_{E} bin where the data are underestimated by the Kr and BFGW calculations.

The situation is rather different for the b and gluon jet fragmentation functions (Figs. 1b) and 1c)) where the description of the data by the NLO predictions is worse and where there are significant differences between individual NLO results, the latter being expected due to differences in the calculations as discussed in [13]. In Fig. 1b) the KKP prediction is deficient with respect to the data for $x_{\mathrm{E}} > 0.12$. In this context, it is important to note that B hadron decay products are indirectly included in theory predictions since they are present in the data sets to which the fits were made.

For the gluon jet fragmentation functions, the two alternative methods of identifying gluon jets described above are examined, see Fig. 1c). The $Q_{\mathrm{j}et}$ binning is not the same for the two methods because of their different regions of applicability. A satisfactory correspondence between the b-tag and energy-ordering methods is found in the entire scale range accessible. The data tend to show larger scaling violations than predicted by any of the calculations.

The results for the flavour inclusive jet fragmentation functions, presented in Fig. 1d), are seen to be consistent with published unbiased jet data from lower energy $\mathrm{e}^+\mathrm{e}^-$ experiments (TASSO, MARK II, TPC and AMY) [6] and previous OPAL results [22,23,24]. The data are also compared to the NLO predictions of KKP, Kr and BFGW which all give a reasonable description of the data in the region of $0.06 < x_{\mathrm{E}} < 0.60$ and over the entire scale range.

A good correspondence found between the results from biased and unbiased jets in all four figures suggests that Q_{jet} is an appropriate choice of scale in three-jet events with a general topology. A similar conclusion was previously made in [5]. The MC study presented in [13], however, demonstrates that the bias introduced in the gluon jet identification is not negligible for $x_{\mathrm{E}} > 0.6$. In each of these figures, the scaling violation seen in the data is positive for low x_{E} and negative for high x_{E}. It is more pronounced in the gluon jets than in the quark jets.

References

1. S.J. Brodsky and J.F. Gunion, Phys. Rev. Lett. **37** (1976) 402; K. Konishi, A. Ukawa and G. Veneziano, Phys. Lett. **B78** (1978) 243.
2. OPAL Coll., G. Alexander *et al.*, Phys. Lett. **B265** (1991) 462; OPAL Coll., P. Acton *et al.*, Z. Phys. **C58** (1993) 387; OPAL Coll., R. Akers *et al.*, Z. Phys. **C68** (1995) 179; DELPHI Coll., P. Abreu *et al.*, Z. Phys. **C70** (1996) 179; ALEPH Coll., D. Buskulic *et al.*, Phys. Lett. **B384** (1996) 353.
3. ALEPH Coll., D. Buskulic *et al.*, Phys. Lett. **B346** (1995) 389.
4. OPAL Coll., G. Abbiendi *et al.*, Eur. Phys. J. **C11** (1999) 217.
5. DELPHI Coll., P. Abreu *et al.*, Eur. Phys. J. **C13** (2000) 573.
6. TASSO Coll., Z. Phys. **C 47** (1990) 187; MARK II Coll., A. Peterson *et al.*, Phys. Rev. **D37** (1998) 1; TPC Coll., H. Aihara *et al.*, Phys. Rev. Lett. **61** (1988) 1263; AMY Coll., Y.K. Li *et al.*, Phys. Rev. **D41** (1990) 2675.
7. DELPHI Coll., P. Abreu *et al.*, Eur. Phys. J. **C5** (1998) 585.
8. OPAL Coll., K. Ackerstaff *et al.*, Eur. Phys. J. **C7** (1999) 369.
9. CLEO Coll., M.S. Alam *et al.*, Phys. Rev. **D46** (1992) 4822; CLEO Coll., M.S. Alam *et al.*, Phys. Rev. **D56** (1997) 17.
10. OPAL Coll., G. Alexander *et al.*, Phys. Lett. **B388** (1996) 659; OPAL Coll., K. Ackerstaff *et al.*, Eur. Phys. J. **C1** (1998) 479.
11. OPAL Coll., G. Abbiendi *et al.*, Eur. Phys. J. **C23** (2002) 597.
12. OPAL Coll., G. Abbiendi *et al.*, Phys. Rev. **D69** (2004) 032002.
13. OPAL Coll., G. Abbiendi *et al.*, submitted to Eur. Phys. J., hep-ex/0404026.
14. S. Catani *et al.*, Phys. Lett. **B269** (1991) 432.
15. Yu.L. Dokshitzer *et al.*, JHEP **9708** (1997) 001.
16. UA1 Coll., G. Arnison *et al.*, Phys. Lett. **B122** (1983) 103; J.E. Huth *et al.*, Ed. E.L. Berger, World Scientific, Singapore (1990) 134; OPAL Coll., R. Akers *et al.*, Z. Phys. **C63** (1994) 197.
17. ALEPH Coll., D. Buskulic *et al.*, Z. Phys. **C76** (1997) 191.
18. Yu. Dokshitzer *et al.*, Basics of perturbative QCD, Editions Frontières (1991).
19. B.A. Kniehl, G. Kramer and B. Pötter, Nucl. Phys. **B582** (2000) 514.
20. S. Kretzer, Phys. Rev. **D62** (2000) 054001.
21. L. Bourhis *et al.*, Eur. Phys. J. **C19** (2001) 89.
22. OPAL Coll., G. Alexander *et al.*, Z. Phys. **C72** (1996) 191.
23. OPAL Coll., K. Ackerstaff *et al.*, Z. Phys. **C75** (1997) 193.
24. OPAL Coll., G. Abbiendi *et al.*, Eur. Phys. J. **C16** (2000) 185.

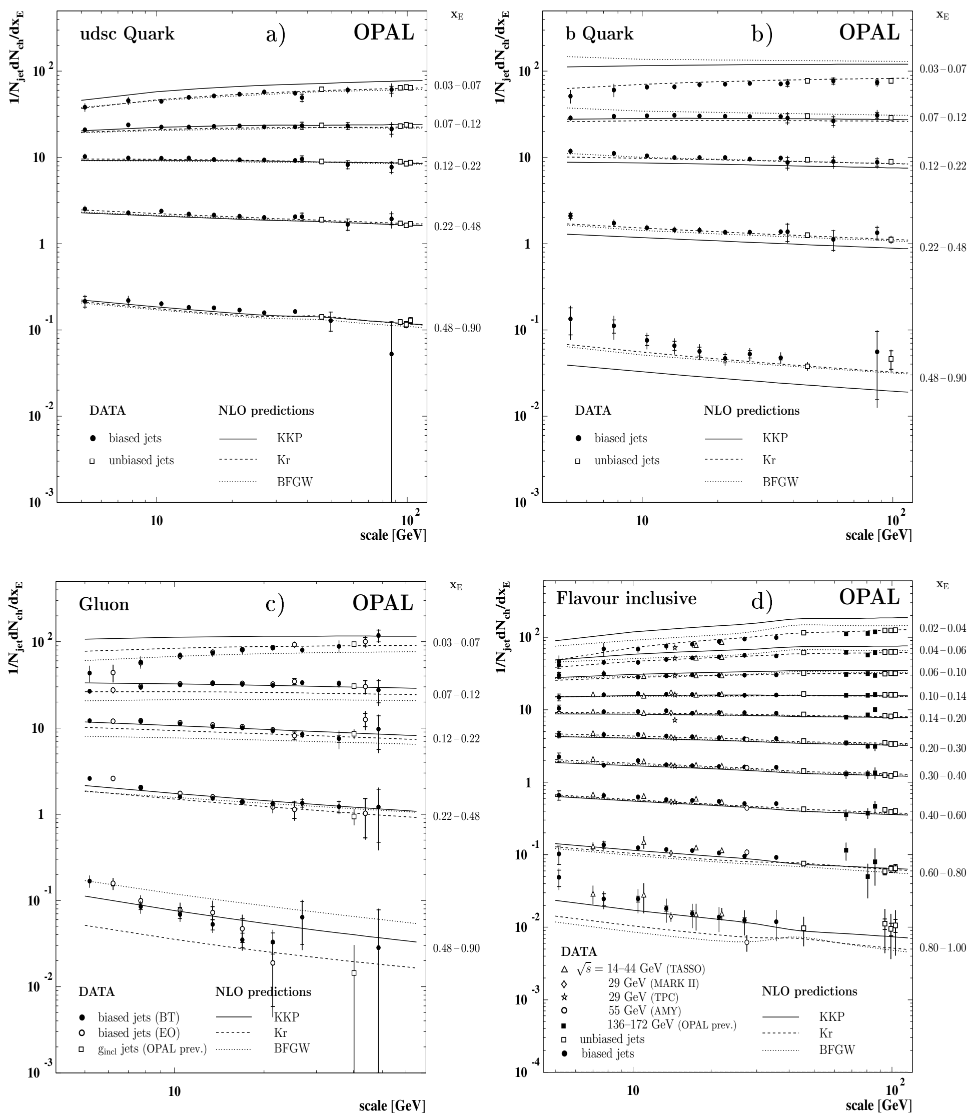

Figure 1: Scale dependence of fragmentation functions in different $x_{\rm E}$ bins. The scale denotes Q_{jet} for the biased jets and $\sqrt{s}/2$ for the unbiased jets. The inner error bars indicate the statistical uncertainties, the total error bars show the statistical and systematic uncertainties added in quadrature. The data are compared to the NLO predictions by KKP [19], Kr [20] and BFGW [21]. a) udsc jets, b) b jets, c) gluon jets from b-tag (BT) method and energy-ordering (EO) method. In addition, the published g_{incl} jets [4] are shown at $E_{\rm jet} = 40.1$ GeV. d) flavour inclusive jets. In addition, the published unbiased jet data by TASSO, TPC, MARK II, AMY [6] and OPAL [22,23,24] are shown.